

Factorial Design and Evaluation of the Influence of Cu²⁺ Salts Counterions on the Synthesis of MOF 199

Ivan Henrique Silva Amorim^a, Patricia Figueiredo Santos^a, Paulo Roberto Filgueiras^a, and Priscilla Paiva Luz^{a*}

Universidade Federal do Espírito Santo, 514 Fernando Ferrari Av., Vitória, 29075-910, Brazil.

Article history: Received: 07 August 2018; revised: 31 October 2018; accepted: 31 October 2018. Available online: 31 December 2018. DOI: <http://dx.doi.org/10.17807/orbital.v10i7.1213>

Abstract:

This work aimed to evaluate the influence of Cu²⁺ salts counterions (acetate and chloride) and the synthesis conditions on the reaction yield of MOF-199, a well-known metalorganic framework. Therefore, a factorial design was performed for this purpose in which three reaction parameters were analyzed: temperature, time and metal concentration, varying in two levels (minimum and maximum), resulting in a combinatorial analysis, where each experiment consisted in a different configuration of the factors at their respective levels, which led to a batch of 23 = 8 experiments, for each Cu²⁺ salt. Syntheses with average values of each parameter were also performed, totaling 9 experiments for each counterion. Reaction yield was the factorial design response variable and the products were characterized by infrared vibrational spectroscopy, thermogravimetric analysis and powder X-ray diffraction. Analytical techniques confirmed the production of MOF-199 and the proposed statistic model of the response variable showed good agreement with the experimental values. In addition, the temperature parameter was the only significant variable on the reaction yields for the syntheses with Cu²⁺ chloride. The syntheses carried out with Cu²⁺ acetate provided higher yields compared to Cu²⁺ chloride, however the evaluated synthesis conditions were not significant.

Keywords: counterion; Cu²⁺ ion; factorial design; metalorganic framework; MOF-199; trimesic acid

1. Introduction

Metalorganic frameworks (MOFs) consist of a class of compounds on the rise and have been extensively studied in recent years due to their various interesting properties and consequently numerous applications. MOFs consist of crystalline and robust structure materials, geometrically well defined, resulting from the coordination of organic ligands to metal ions or clusters, polymerizing and forming a coordination network containing potential voids [1]. Each ligand, together with the metal, is responsible for imparting specific properties to each MOF in terms of structure and functionality [2, 3, 4, 5]. Cavities are formed along the framework structure, which may also be called pores and those are able to capture small molecules and are therefore useful for reaction catalysis [6,7],

molecular adsorption [8], gas separation and storage [9,10,11,12], drugs delivery [13], antibacterial activity [14], precursor for electrode materials [15] and in plant hormones absorption improvement [16], etc.

The first synthesized MOF was MOF-5, composed by Zn²⁺ and 1,4-benzenedicarboxylic acid. However, the lack of active sites available in zinc ions limited the material applications and a Cu²⁺-based MOF seemed to solve that problem. MOF-199, also known as HKUST-1, was firstly synthesized by Chui and coworkers and it consists of a metalorganic framework composed by Cu²⁺ ion and 1,3,5-benzenetricarboxilic acid (BTC) ligand, also known as trimesic acid [17]. The presence of metal-containing clusters with coordinative vacancies, in this case, Cu²⁺, makes MOF-199 capable of binding smaller molecules for both carrying and transportation, or catalyzing

*Corresponding author. E-mail: priscilla.luz@ufes.br

reactions. In its structure, Cu^{2+} form dimers, where each Cu^{2+} atom is coordinated to four oxygen atoms, coming from the carboxylate groups of BTC linkers, and to one water molecule. The presence of water molecules suggests the possibility to obtain a coordinative vacancy on the metal ions species, by dehydration, leading the material to have potential activities in catalysis [17,18].

There are distinct methodologies reported in literature concerning MOF-199 synthesis, which can be, for example, solvothermal, hydrothermal, or dripping with magnetic stirring. In addition, Cu^{2+} :BTC proportion, reaction medium, time, temperature and reagent concentration are also distinct. Cao et al. [11], for instance, produced MOF-199 by adding Cu^{2+} nitrate (17.1 mmol) dissolved in water into a solution of trimesic acid (9.5 mmol) dissolved in ethanol:DMF 1:1 (v/v) and then transferred the final mixture to a solvothermal vial to react for 10 hours at 100 °C. Nguyen et al. [7], in turn, dissolved both the metal salt Cu^{2+} nitrate (1.81 mmol) and the BTC ligand (1.12 mmol) at the same time in a solvent mixture of ethanol:DMF:water (4:3:2 v/v) in a 20 mL vial, which was then heated at 85 °C in an isothermal oven for 24 hours. Khan et al. [15] dissolved Cu^{2+} nitrate (3.0 mmol) in DMF and then added it dropwise on a suspension of trimesic acid ligand (1.0 mmol) in DMF containing triethylamine under stirring at room temperature. These mentioned procedures did not evaluate the influence of the experimental parameters on the reaction yield, for example, and several recent works reported the synthesis optimization based on a factorial design of experiment with different level and factors, such as: sonication time, initial concentration and adsorbent dose for obtaining optimum parameters for copper and lead ions removal by a MOF of cadmium and terephthalate, Cd-TPA, in two levels (2^3) [19]. Similarly, interactive effects among the key synthesis parameters such as drying time, calcination temperature, stirring speed and mass of CaCO_3 were investigated in two levels (2^4) to achieve the highest yield of supported bimetallic (Fe-Co/CaCO_3) catalyst synthesis [20]. Another factorial design (2^2) was developed to study the crystallization time and temperature of the MCM-48 mesoporous materials synthesis, to analyze the specific area of compounds in two levels [21]. Finally, the influence of absorbed dose, reaction time and

monomer concentration over the synthesis of polypropylene-g-poly(glycidylmethacrylate), a functional material for metal ion adsorption, was tested by a factorial design (4^3) [22].

Based on the variety of experimental procedures reported or producing MOF-199 and the absence of information in literature concerning the importance of understanding the significant experimental conditions for MOF-199 production, the aim of this work was to apply a 2^3 factorial design to evaluate the influence of Cu^{2+} salts counterions, acetate (OAc^-) and chloride (Cl^-), and the synthesis parameters (time, temperature and metal concentration) on the reaction yield (response variable) of MOF-199. The obtained compounds were characterized by infrared vibrational spectroscopy (FT-IR spectroscopy), thermogravimetric analysis (TGA) and powder X-ray diffraction (XRD).

2. Results and Discussion

MOF-199 presents two different Cu^{2+} ion coordination spheres, depending on the presence or absence of water molecules coordinated to Cu^{2+} . Literature reports $[\text{Cu}_3(\text{BTC})_2 \cdot 3\text{H}_2\text{O}]$ units, a turquoise form of MOF-199 containing terminal axial *aqua* ligands (Figure 1), and dark blue form obtained after a dehydration processes of $[\text{Cu}_3(\text{BTC})_2 \cdot 3\text{H}_2\text{O}]$ units, without coordinating water molecules [17, 18, 23]. In this work, all 18 obtained compounds were dried up under vacuum at 80 °C during 7 days and the bluish color was the first evidence leading us to conclude those were all MOF-199 containing terminal axial *aqua* ligands. The reaction yields were calculated based on $[\text{Cu}_3(\text{BTC})_2 \cdot 3\text{H}_2\text{O}]$ formula.

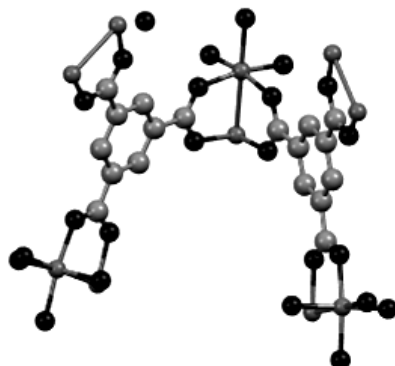


Figure 1. Hydrate MOF-199 structure obtained and determined by Chui et al [17]. Cu^{2+} (dark grey balls), O (black balls) and C (light grey balls).

In addition to the color, the characterization techniques were important to confirm the successful coordination of Cu^{2+} to BTC molecules and the presence of water coordinated to Cu^{2+} . Compound 9 (Cl^-) and Compound 9 (OAc) were chosen as representative of all other synthesized compounds, since all results were similar between them. Free BTC was used as reference for FT-IR spectroscopy and TGA.

2.1. FT-IR spectroscopy

FT-IR spectra of free BTC ligand, Compound 9 (Cl^-) and Compound 9 (OAc) are shown in Figure 2. Bands from 3300 to 2400 cm^{-1} correspond to OH stretching from BTC carboxyl group, as can be seen in the ligand spectrum. This is characteristic of carboxyl group, which tends to strongly interact through hydrogen bonds forming a kind of dimers on solid state. However, in the synthesized compounds spectra those small dimer-like bands were replaced by a single broadband, indicating that the dimer-like form was lost, being an evidence of BTC coordination to Cu^{2+} [7,12]. The synthesized compounds were blue-colored and, according to the literature, it is an evidence of water coordinated to Cu^{2+} . According to the literature, free water exhibits symmetric and asymmetric stretching vibration modes at 3652 and 3756 cm^{-1} , respectively. Since the synthesized compounds spectra exhibit a stretching band around 3345 cm^{-1} , it can be an evidence of coordinated water [24]. Another evidence of BTC coordination to Cu^{2+} was the replacement of C=O stretching from free BTC carboxyl group at 1690 cm^{-1} by characteristic C-O symmetric and asymmetric stretches of carboxylate ion at 1370 and 1640 cm^{-1} , respectively, from deprotonated and coordinated BTC. FT-IR spectra of synthesized compounds are in agreement with those related by Nguyen et al. [7], supporting the evidence of MOF-199 production in this work.

2.2. TGA

Free BTC and synthesized compounds TGA curves are shown in Figure 3. Free BTC thermogram displayed a single weight loss starting at 300°C due to its thermal decomposition. There was no residue formation, as expected for an oxidizing atmosphere. The

production of MOF-199 was also confirmed by TGA, since the synthesized compounds thermograms exhibited a weight loss up to 100 °C attributed to coordinated water molecules. From 100 to 200 °C there was the removal of DMF molecules located in the pores. Afterwards, there was an intense mass loss corresponding to coordinated BTC thermal decomposition. At 320 °C residual mass was observed and it can be attributed to CuO , since the TGA was performed under oxidizing atmosphere. Cao et al. [11] also performed TGA for MOF-199 and their achievements are similar to the results exhibited in Figure 3, reinforcing success on MOF-199 formation.

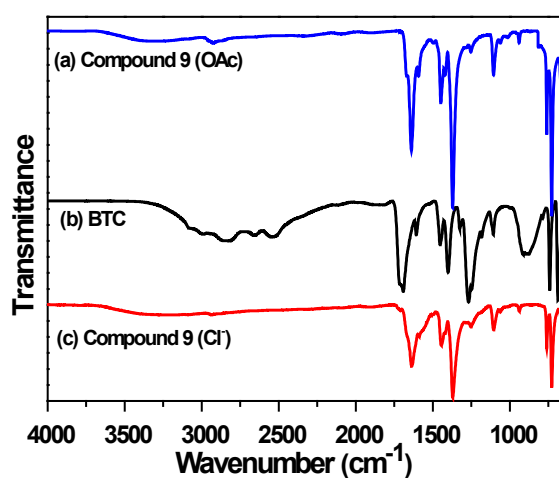


Figure 2. FT-IR spectra of (a) Compound 9 (OAc), (b) BTC and (c) Compound 9 (Cl $^-$).

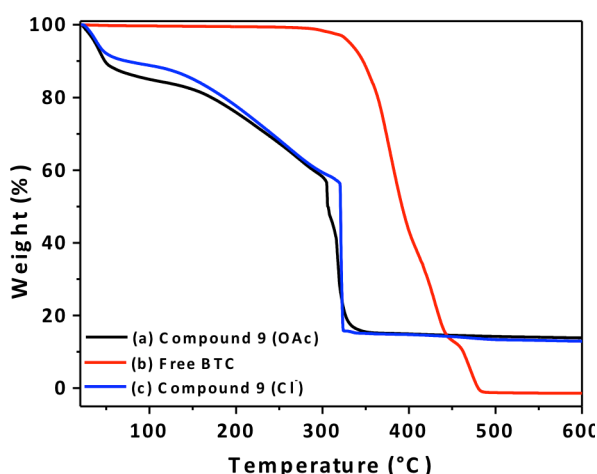


Figure 3. TGA curves of (a) Compound 9 (OAc), (b) free BTC and (c) Compound 9 (Cl $^-$).

2.3. XRD

Compound 9 (OAc) and Compound 9 (Cl⁻) X-ray diffractograms are shown in Figure 4. The main peaks appear at $2\theta = 6.6^\circ, 9.5^\circ, 11.7^\circ, 13.5^\circ, 19.0^\circ$ and 26.0° , which are in agreement with previous reports concerning MOF-199 synthesis [7,11, 25], a final indication of successful MOF-199 production. The cell parameters for these compounds were in agreement with previous reported literature [17, 26]. According to Chui et al, in MOF-199 Cu²⁺ ions form dimers, where each Cu²⁺ ion is coordinated by four oxygens, coming from BTC linkers and by one water molecule (Figure 1) [17].

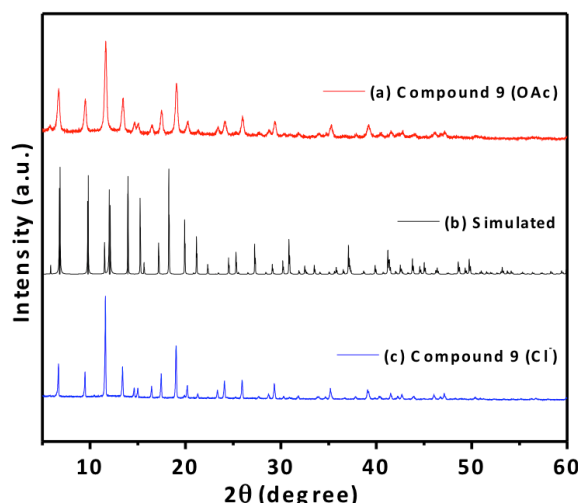


Figure 4. Powder XRD patterns of (a) Compound 9 (OAc), (b) simulated data from the deposited structure [17] and (c) Compound 9 (Cl⁻).

2.4. Factorial design

According to XRD results, reaction yields of all 18 compounds were calculated based on hydrate MOF-199 structure (Figure 1) and the results are listed in Table 1. As can be seen, acetate and

chloride played an important influence over MOF-199 production, with acetate ion contributing for considerable higher yields for all reaction conditions compared to those reaction yields with chloride as anion. This difference may be due to the fact that acetate ion is derived from a weak acid and, as a consequence, it is a stronger conjugate Brønsted base than chloride ion, which comes from a strong acid. As a stronger base, acetate ion plays a greater tendency to abstract the hydrogen atom from BTC carboxyl group, thus favoring BTC coordination to Cu²⁺ [27].

Table 1. Reaction yields for each synthesized compound.

Compound	Cu ₃ (BTC) ₂ ·3H ₂ O Yield (acetate) (%)	Cu ₃ (BTC) ₂ ·3H ₂ O Yield (chloride) (%).
1	18.48	5.85
2	42.15	1.36
3	43.56	2.43
4	55.05	0.12
5	49.25	13.26
6	48.23	10.22
7	46.97	18.11
8	46.34	15.05
9	37.35	2.91

2.4.1. Compounds synthesized from Cu²⁺ acetate factorial design

For the analysis of Cu²⁺ acetate, a model was built (described on item 3.) with interactions between two factors and a coefficient of determination (R^2) of 93.56% was obtained. From Table of Effects (Table 2) it was possible to observe the influence of each factor on the response variable and the interaction between the factors.

Table 2. Table of Effects for compounds synthesized from Cu²⁺ acetate.

Factor	Effect	Coefficient	Std. Err.	t(2)*	p**
Mean/interactions	43.0422	43.04	1.77	24.36	0.002
(1) Concentration (mol L ⁻¹)	8.3775	4.19	3.75	2.23	0.155
(2) Time (min)	8.4525	4.23	3.75	2.25	0.153
(3) Temperature (°C)	7.8875	3.94	3.75	2.10	0.170
(1*2) Concentration*Time	-2.9475	-1.47	3.75	-0.79	0.514
(1*3) Concentration*Temperature	-9.2025	-4.60	3.75	-2.46	0.133
(2*3) Time*Temperature	-10.5375	-5.27	3.75	-2.81	0.107

*Student-test; ** p-value.

Only the mean was shown to be significant. Concentration, time and temperature factors have an increasing effect on the response variable. Interactions between the factors have a decreasing effect on the response variable

(negative values), which means the variables are antagonistic and the surface graphics confirm this analysis (Figure 5). However, concentration, time and temperature at higher level increased the reaction yield.

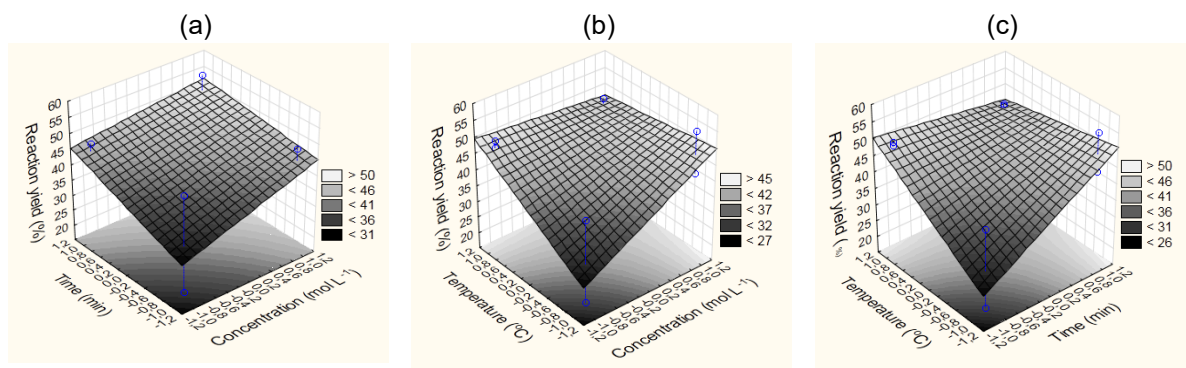


Figure 5. Surface Graphics for compounds synthesized from Cu^{2+} acetate. (a) Concentration x Time x Yield, (b) Concentration x Temperature x Yield, (c) Time x Temperature x Yield.

The coefficients values allowed fitting a regression model based on:

$$\hat{y}(x_1, x_2, x_3) = 43.04 + 4.19x_1 + 4.23x_2 + 3.94x_3 - 1.47x_1x_2 - 4.60x_1x_3 - 5.27x_2x_3 \quad \text{Eq.1}$$

The obtained yield (response variable) for Cu^{2+} acetate syntheses showed good proximity with the predicted yield, as presented in Figure 6, indicating a good agreement to the model. Although the controlled factors are not significant, the proposed model responds well to the yield.

The significance coefficients of the model (Eq.1) were evaluable by Student t-test with significance level of 5%. For $\alpha = 5\%$, p-value values lower than 5% are significant to the response variable. In the ANOVA Table (Table 3) it is seen that p-value values are higher than 5% for all factors and interactions, inferring that they

are not significant to the response variable.

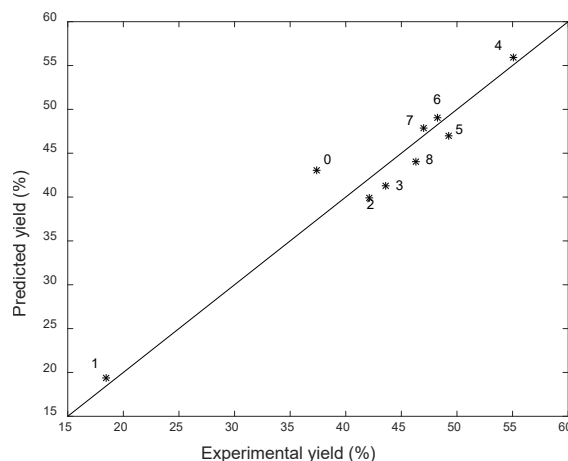


Figure 6. Experimental yield against predicted yield for compounds synthesized from Cu^{2+} acetate determined by Eq.1.

Table 3. Table ANOVA for compounds synthesized from Cu^{2+} acetate.

Factor	SS	df	MS	F*	p**
(1) Concentration (mol L⁻¹)	140.3650	1	140.3650	5.00	0.155
(2) Time (min)	142.8895	1	142.8895	5.08	0.153
(3) Temperature (°C)	124.4253	1	124.4253	4.43	0.170
(1*2) Concentration*Time	17.3755	1	17.3755	0.62	0.514
(1*3) Concentration*Temperature	169.3720	1	169.3720	6.03	0.133
(2*3) Time*Temperature	222.0778	1	222.0778	7.90	0.107
Residual	56.2022	2	28.1011		
Total SS	872.7074	8			

*Fisher-Snedecor F-test, ** p-value.

2.4.2. Compounds synthesized from Cu^{2+} chloride factorial design

For the analysis of Cu^{2+} chloride (described on item 3), with interactions between two factors, $R^2 = 92.48\%$ was obtained. Table of Effects (Table 4)

presented the influence of each factor on the response variable and the interactions between the factors.

Table 4. Table of Effects for compounds synthesized from Cu^{2+} chloride.

Factor	Effect	Coefficient.	Std. Err.	t(2)*	p**
Mean/interactions	7.70111	7.70	1.21	6.36	0.024
(1) Concentration (mol L ⁻¹)	-3.22500	-1.61	2.57	-1.25	0.336
(2) Time (min)	1.25500	0.63	2.57	0.49	0.674
(3) Temperature (°C)	11.72000	5.86	2.57	4.56	0.045
(1*2) Concentration*Time	0.54000	0.27	2.57	0.21	0.853
(1*3) Concentration*Temperature	0.17500	0.09	2.57	0.07	0.952
(2*3) Time*Temperature	3.58500	1.79	2.57	1.39	0.298

*Student t-test; ** p-value.

From Table 4 it is possible to observe that concentration factor had a decreasing effect on the response variable, while temperature, time and the interactions between the factors had an increasing effect on the response variable, which

means the variables are synergistic. Surface graphics confirmed this statement (Figure 7). For higher temperature and time values, the yield increases and for higher concentration values the yield decreases.

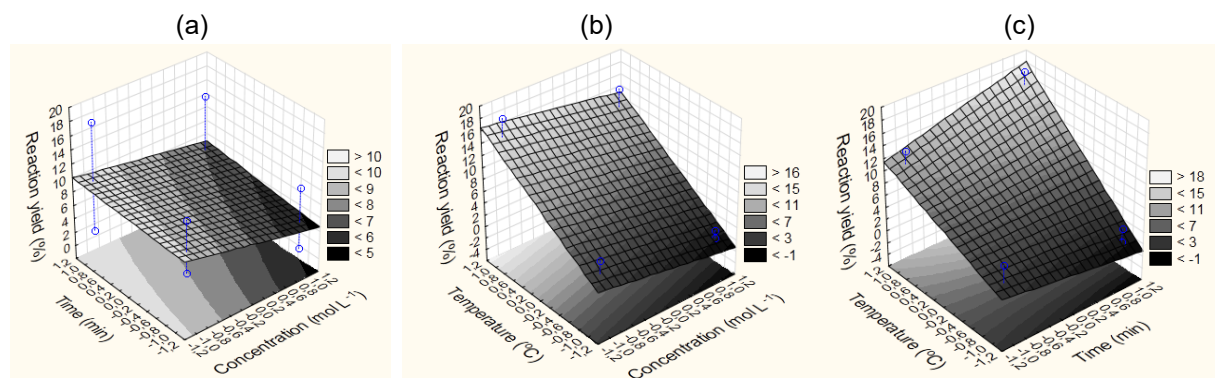


Figure 7. Surface Graphics for compounds synthesized from Cu^{2+} chloride. (a) Concentration x Time x Yield, (b) Concentration x Temperature x Yield, (c) Time x Temperature x Yield.

The coefficients values allowed fitting a regression model based on:

$$\hat{y}(x_1, x_2, x_3) = 7.70 - 1.61x_1 + 0.63x_2 + 5.86x_3 + 0.27x_1x_2 + 0.09x_1x_3 + 1$$

Eq.2

The obtained yield (response variable) for Cu^{2+} chloride syntheses showed good proximity with the predicted yield, as presented in Figure 8, indicating a good response with the model. Only the central point estimated presented a residue higher than expected.

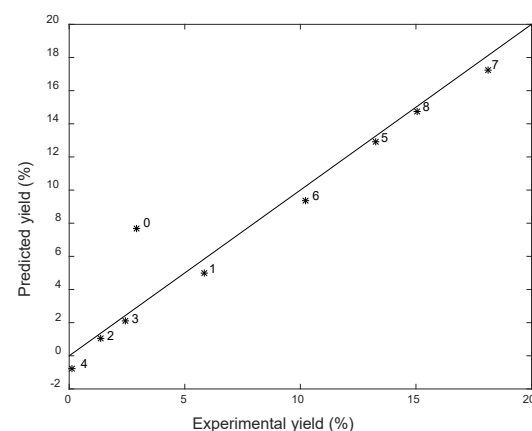


Figure 8. Experimental yield against predicted yield for compounds synthesized from Cu^{2+} chloride determined by Eq.2.

In the ANOVA Table (Table 5) it is seen that only the temperature factor has a p-value lower than 5%, whereas other factors and their

interactions have a p-value higher than 5%, which means only the temperature was significant to the response variable.

Table 5. Table ANOVA for compounds synthesized from Cu²⁺ chloride.

Factor	SS	df	MS	F*	p**
(1) Concentration (mol L ⁻¹)	20.8013	1	20.8013	1.57	0.336
(2) Time (min)	3.1500	1	3.1500	0.24	0.674
(3) Temperature (°C)	274.7168	1	274.7168	20.79	0.045
(1*2) Concentration*Time	0.5832	1	0.5832	0.04	0.853
(1*3) Concentration*Temperature	0.0613	1	0.0613	<0.01	0.952
(2*3) Time*Temperature	25.7045	1	25.7045	1.95	0.298
Residual	26.4291	2	13.2145		
Total SS	351.4461	8			

* Fisher-Snedecor F-test; ** p-value.

3. Material and Methods

3.1. Materials

Absolute ethanol (99.8%), Cu(OAc)₂.H₂O and CuCl₂.2H₂O, both P.A. grade, were purchased from VETEC®, BTC (95%) was provided by ALDRICH®, and DMF (P.A. grade) was obtained from Scientific Exodus®.

3.2. Factorial Design description

For the synthesis of MOF-199, a two-leveled (lower (-) and upper (+) levels) full factorial design was performed in order to study the influence and

the interaction of the reaction variables on the reaction yield (response variable). The adopted procedures, as well as synthetic conditions, were chosen based on previous MOF-199 reported literature [2, 7, 9, 11, 12, 15, 25]. Thus, the reaction conditions (variables or factors) studied were: metal concentration, time and temperature. Being three variables studied at two levels, plus the variables average values, nine experiments, for each counterion (acetate and chloride), were performed combining those parameters. The expected response of the factorial design was the synthesis yields. The lower and upper values for each variable are listed in Table 6.

Table 6. Factorial design variables and their respective values for lower (-) and upper (+) levels.

Variables / Levels	Lower (-)	Upper (+)
Concentration (mol L ⁻¹)	1.7 x 10 ⁻²	3.5 x 10 ⁻²
Time (min)	60	120
Temperature (°C)	25	78

78 °C was chosen as temperature upper level since it is the boiling point of ethanol, one of the solvents used in the reactions. In addition, synthesis at higher temperatures can lead to formation of MOFs without ancillary ligands [28].

3.3. Experimental procedure

In terms of experimental methodology, all syntheses of the factorial design proceeded in a very similar way, differing from each other on the pre-established values of the studied factors. The random sequence of synthesized compounds and

their reaction conditions are shown in Table 7.

0.5 mL of a Cu²⁺ aqueous solution (concentration described at Table 6) was added to a BTC ethanol/DMF 1:1 (v/v) solution (1.9 10⁻²mol L⁻¹ and 3.8 10⁻²mol L⁻¹ for lower and upper level, respectively) drop wise by using a 500 µL micropipette every 2 minutes for a total of 20 minutes of addition time (not taking in account for the reaction time parameter), under magnetic stirring, at 25 or 78 °C, and during 60 or 120 min. The dark blue solids were washed with an ethanol:DMF:water (1:1:1) mixture, dried at vacuum for 1 week at 80 °C, and characterized by

FT-IR spectroscopy, XRD and TGA.

Table 7. Synthesized compounds and their respective combination of factor levels, where the upper level is represented by (+), the lower level by (-) and the average level as (0).

Compound	Factor 1 (Concentration)	Factor 2 (time)	Factor 3 (temperature)
1	-	-	-
2	+	-	-
3	-	+	-
4	+	+	-
5	-	-	+
6	+	-	+
7	-	+	+
8	+	+	+
9	0	0	0

3.4. Experimental design

Statistical treatment of the reaction yields data was carried out using Statistica software [29]. This statistical treatment is based on the analysis of the influence of each factor (concentration, time and temperature) on the response variable (reaction yield).

The standard error (Std. Err.) was calculated based on prediction error (e) from model:

$$e = y - \hat{y} \quad \text{Eq.3,}$$

where \hat{y} is the yield predicted by model:

$$\hat{y}(x_1, x_2, x_3) = b_0 + b_1 x_1 + b_2 x_2 + b_3 x_3 + b_{12} x_1 x_2 + b_{13} x_1 x_3 + b_{23} x_2 x_3 \quad \text{Eq.4,}$$

being b the reaction parameters coefficient, x_1 = metal concentration; x_2 = reaction time; x_3 = temperature and $x_1 x_2$, $x_1 x_3$, $x_2 x_3$ the interaction between those factors. Sum of squares (SS) error was determined by:

$$SS = \sum e^2 \quad \text{Eq.5,}$$

then:

$$SS = \sum (y - \hat{y})^2 \quad \text{Eq.6.}$$

The experimental variance estimative was performed by mean squares residual MS_{residual} : from analysis of variance (ANOVA) of the residuals model:

$$MS_{\text{residual}} = SS / \sqrt{df} \quad \text{Eq.7,}$$

where df is the number of degree of freedom of the residuals, determined by:

$$df = n - d \quad \text{Eq.8,}$$

where n and d are the number of samples ($n = 9$)

and coefficients model ($d = 7$).

The square root of MS_{residual} is a good estimative for the standard deviation model. Thus, the standard error was calculated by:

$$Std. Err. = \sqrt{MS_{\text{residual}}} / \sqrt{df} \quad \text{Eq.9.}$$

Standard error was used to determine the significance of coefficients model b's.

3.5. Characterization

Infrared spectroscopy analysis was performed with Spectrum 400 FT-MIR / FT-NIR - Perkin Elmer®, in attenuated total reflectance (ATR) mode, 16 scans, with a resolution of 4 cm^{-1} . TGA was conducted with a SDT Q600 - TA Instruments®. Analyses were done under synthetic air atmosphere at a flow rate of 50 mL min^{-1} , at a heating rate of $10 \text{ }^{\circ}\text{C min}^{-1}$, from room temperature to $600 \text{ }^{\circ}\text{C}$. Powder X-ray diffraction (XRD) patterns were taken on a D8 Discover - Bruker® using $\text{Cu K}\alpha$ radiation ($\lambda = 0.15406 \text{ nm}$). The tube voltage was 40 kV and the current was 30 mA . XRD diffraction patterns were taken in 2θ range of $5 - 70^{\circ}$ at a scan speed of $2^{\circ} \text{ min}^{-1}$.

4. Conclusions

FT-IR spectra, TGA and XRD were important to confirm the formation of MOF-199. The proposed statistic model was robust within the investigated range for these three variables. Although most of the factors presented no significance, the model showed good response, since the experimental yield value was close to

the predicted yield value. For Cu^{2+} acetate, isolated studied variables increased the reaction yield, but it was not significant and the interactions between the factors were antagonistic. Nevertheless, the temperature showed the most positive influence over the response variable for the syntheses using Cu^{2+} chloride, being the only significant factor and the interaction between the variables were synergistic. In addition, the syntheses using Cu^{2+} acetate showed much higher yields than those syntheses performed with Cu^{2+} chloride.

Acknowledgments

I. H. S. Amorim gratefully thank Coordenação de Aperfeiçoamento de Pessoal de Nível Superior (CAPES) for scholarship. All authors thank Núcleo de Competências em Química do Petróleo (NCQP) for IR, TG and X-Ray analyses.

References and Notes

- [1] Öhrström, L. *Crystals* **2015**, *5*, 154. [\[Crossref\]](#)
- [2] Ferey, G. *Chem. Soc. Rev.* **2008**, *37*, 191. [\[Crossref\]](#)
- [3] Hoskins, B. F.; Robson, R. *J. Am. Chem. Soc.* **1989**, *111*, 5962. [\[Crossref\]](#)
- [4] Tranchemontagne, D. J.; Mendoza-Cortes, J. L.; O'Keeffe, M.; Yaghi, O. M. *Chem. Soc. Rev.* **2009**, *38*, 1257. [\[Crossref\]](#)
- [5] Batten, S. R.; Champness, N. R.; Chen, X-M.; Garcia-Martinez, J.; Kitagawa, S.; Öhrström, L.; O'Keeffe, M.; Suh, M. P.; Reedijk, J. *Pure Appl. Chem.* **2013**, *85*, 1715. [\[Crossref\]](#)
- [6] Loera-Serna, S.; Ortiz, E. In: *Catalytic Applications of Metal-Organic Frameworks*. Luis, N., ed. London: IntechOpen, 2016, chapter 4. [\[Crossref\]](#)
- [7] Nguyen, L. T.L.; Nguyen, T. T.; Nguyen, K. D.; Phan, N. T. S. *Appl. Catal., A: General* **2012**, *425*, 44. [\[Crossref\]](#)
- [8] Wang, X. L.; Jin, L.; Lin, H. Y.; Hu, H. L.; Chen, B. K.; Bao, M. *Solid State Sci.* **2009**, *11*, 2118. [\[Crossref\]](#)
- [9] Pinto, M. S.; Serra-Avila, C. A.; Hinestroza, J. P. *Cellulose* **2012**, *19*, 1771. [\[Crossref\]](#)
- [10] Banerjee, D.; Simon, C. M.; Plonka, A. M.; Motkuri, R. K.; Liu, J.; Chen, X.; Smit, B.; Parise, J. B.; Haranczyk, M.; Thallapally, P. K. *Nat. Commun.* **2015**, *7*, 11831. [\[Crossref\]](#)
- [11] Cao, Y.; Zhao, Y.; Song, F.; Zhong, Q. *J. Energy Chem.* **2014**, *23*, 468. [\[Crossref\]](#)
- [12] Thi, T. V. N.; Luu, C. L.; Hoang, T. C.; Nguyen, T.; Bui, T. H.; Nguyen, P. H. D.; Thi, T. P. P. *Adv. Nat. Sci.: Nanosci. Nanotechnol.* **2013**, *4*, 035016. [\[Crossref\]](#)
- [13] Keskin, S.; Kızılel, S. *Ind. Eng. Chem. Res.* **2011**, *50*, 1. [\[Crossref\]](#)
- [14] Rodríguez, H. S.; Hinestroza, J.P.; Ochoa-Puentes, C.; Sierra, C. A.; Soto, C. Y. *J. Appl. Polym. Sci.* **2014**, *131*, 40815. [\[Crossref\]](#)
- [15] Khan, I. A.; Badshah, A.; Nadeem, M. A.; Haider, N.; Nadeem, M.A. *Int. J. Hydrogen Energy* **2014**, *39*, 19609. [\[Crossref\]](#)
- [16] Zhang, Z.; Huang, Y.; Ding, W.; Li, G. *Anal. Chem.* **2014**, *86*, 3533. [\[Crossref\]](#)
- [17] Chui, S. S. Y.; Lo, S. M. F.; Charmant, J. P. H.; Orpen, G.; Williams, I. D. *Sci.* **1999**, *283*, 1148. [\[Crossref\]](#)
- [18] Prestipino, C.; Regli, L.; Vitillo, J. G.; Bonino, F.; Damin, A.; Lamberti, C.; Zecchina, A.; Solari, P. L.; Kongshaug, K. O.; Bordiga, S. *Chem. Mater.* **2006**, *18*, 1337. [\[Crossref\]](#)
- [19] Ghaedi, A. M.; Panahimehr, M.; Nejad, A. R. S.; Hosseini, S. J.; Vafaei, A.; Baneshi, M. M. *Journal of Molecular Liquids*, **2018**, *272*, 15. [\[Crossref\]](#)
- [20] Bankole, M. T.; Mohammed, I. A.; Abdulkareem, A. S.; Tijani, J. O.; Ochigbo, S. S.; Abubakre, O. K.; Afolabi, A. S. *J. Alloys Compd.* **2018**, *749*, 85. [\[Crossref\]](#)
- [21] Nascimento, A. R.; Medeiros, R. L. B. A.; Melo, M. A. F.; Melo, D. M. A.; Souza, M. J. B. *Cerâmica* **2016**, *62*, 413. [\[Crossref\]](#)
- [22] Madrid, J. F.; Lopez, G. E. P.; Abad, L. V. *Radiat. Phys. Chem.* **2017**, *136*, 54. [\[Crossref\]](#)
- [23] Phan, N. T. S.; Nguyen, T. T.; Nguyen, C. V.; Nguyen, T. T. *Appl. Catal. A: General* **2013**, *457*, 69. [\[Crossref\]](#)
- [24] Silverstein, R. M.; Webster, F. X.; Kiemle, D. J. *Spectrometric Identification of Organic Compounds*, 7th ed. New York: John Wiley & Sons, Inc., 2005.
- [25] Wang, S.; Wang, X.; Ren, Y.; Xu, H. *Chromatographia* **2015**, *78*, 621. [\[Crossref\]](#)
- [26] Loera-Serna, S.; Oliver-Tolentino, M. A.; López-Núñez, M. L.; Santana-Cruz, A.; Guzmán-Vargas, A.; Cabrera-Sierra, R.; Beltrán, H. I.; Flores, J. J. *Alloys Compd.* **2012**, *540*, 113. [\[Crossref\]](#)
- [27] Huheey, J. E.; Keiter, A. E.; Keiter, R. L. *Inorganic Chemistry-Principle of Structure and Reactivity*, 4th ed. New York: Harper Collins College Publishers, 1993.
- [28] Haynes, W. M.; *Handbook of Chemistry and Physics*, 92nd ed. Boca Raton, FL: CRC Press, 2011.
- [29] Stat Soft.Inc. (2014). *STATISTICA* (data analysis software system), version 12. www.statsoft.com